

Thermodynamic anomalies in a lattice model of water: Solvation properties

M. Pretti and C. Buzano

*Istituto Nazionale per la Fisica della Materia (INFN) and Dipartimento di Fisica,
Politecnico di Torino, Corso Duca degli Abruzzi 24, I-10129 Torino, Italy*

(Dated: March 19, 2018)

We investigate a lattice-fluid model of water, defined on a 3-dimensional body-centered cubic lattice. Model molecules possess a tetrahedral symmetry, with four equivalent bonding arms. The model is similar to the one proposed by Roberts and Debenedetti [J. Chem. Phys. **105**, 658 (1996)], simplified by removing distinction between “donors” and “acceptors”. We focus on solvation properties, mainly as far as an ideally inert (hydrophobic) solute is concerned. As in our previous analysis, devoted to neat water [J. Chem. Phys. **121**, 11856 (2004)], we make use of a generalized first order approximation on a tetrahedral cluster. We show that the model exhibits quite a coherent picture of water thermodynamics, reproducing qualitatively several anomalous properties observed both in pure water and in solutions of hydrophobic solutes. As far as supercooled liquid water is concerned, the model is consistent with the second critical point scenario.

PACS numbers: 05.50.+q 61.20.-p 65.20.+w 82.60.Lf

I. INTRODUCTION

From the experimental point of view, water is known to exhibit several thermodynamic anomalies^{1,2,3}. Contrary to most fluids, at ordinary pressure the solid phase (ice) is less dense than the liquid phase. The latter displays a temperature of maximum density at constant pressure, while both isothermal compressibility and isobaric heat capacity display a minimum as a function of temperature. Moreover, heat capacity is on average much larger than usual. Anomalous properties of neat water have been studied for long, but much interest has been devoted also to unusual properties of water as a solvent, in particular for nonpolar (hydrophobic) chemical species^{4,5,6,7}. Insertion of a nonpolar solute molecule in water is characterized by positive solvation Gibbs free energy (it is thermodynamically unfavored), negative solvation enthalpy (it is energetically *favoured*), negative solvation entropy (it has an ordering effect), and large positive solvation heat capacity^{8,9}. More precisely, for prototype hydrophobic species (that is, for instance, noble gases), solvation entropies and enthalpies, which are negative at room temperature, increase upon increasing temperature, and eventually become positive. These properties define the so-called hydrophobic effect, whose importance in biological processes, such as protein folding, has been emphasized in the latest years¹⁰.

From the theoretical point of view, one can relate the anomalous properties of neat water to the formation of a large amount of hydrogen bonds, because of peculiar features of water molecules^{11,12}. The same physics is believed to underly the hydrophobic effect^{4,5,13}, but a comprehensive theory which explains all of these phenomena has not been developed yet. A possible way of investigation consists of computer simulations^{14,15,16}, based on very detailed (but still phenomenological) interaction potentials. In this way, quite a high level of accuracy in describing water thermodynamics has been achieved. Nevertheless, simulations are generally limited by the

large computational effort required, while microscopic physical mechanisms are sometimes hidden by a large number of model details. A complementary approach involves investigations of simplified models^{7,17,18,19}. Although quantitative accuracy is sometimes poor, this approach usually allows more detailed analysis, in a wide range of thermodynamic conditions, with relatively low computational cost. One of these attempts is based on the application of scaled-particle theory²⁰ to hydrophobic hydration²¹. A recent descendant of scaled-particle theory is the information theory approach by Pratt and coworkers²², based on previous knowledge of water properties, such as the pair correlation function, which can be obtained by experiments or by simulations. According to the cited studies, the hydrophobic effect would result mostly from small size of water molecules, and not from water structuring by the solute, as in the classical view⁴. Such effect, though existing, would be scarcely relevant for a description of the hydrophobic effect. The simplified molecular thermodynamic theory of Ref. 17 is basically in agreement with this conclusion. Different theories stress that the large positive heat capacity variation, observed upon insertion of apolar solutes into water, can only arise from cooperativity, that is, from induced ordering of water molecules, so that a theory of the hydrophobic effect should be based on a description of this phenomenon. This position is supported by the results of the 2-dimensional “Mercedes Benz” model, first introduced by Ben-Naim in 1971²³, and extensively investigated by Dill and coworkers in the latest years⁷. Contrary to the previously mentioned approaches, the Mercedes Benz model, though involving high simplifications, is based on well defined microscopic interactions, that is, on an energy function, without previous knowledge of water properties. One important reason to do so is the need of modelling water in a computationally convenient way, in order to investigations on complex systems such as biomolecules, for which water plays a key role. An even more simplified approach^{18,24,25}, which

nevertheless can in principle satisfy this criterion, relies on the long standing tradition of lattice fluid models. As far as neat water is concerned, several different models, both in 2^{26,27,28,29,30,31,32,33} and 3 dimensions^{34,35,36,37,38,39,40,41} have been investigated, some of which are variations of the early model proposed by Bell in 1972³⁴. One of them is the 3-dimensional model by Roberts and Debenedetti^{40,42,43}, defined on the body-centered cubic lattice. In this model, water molecules possess four bonding arms (2 donors and 2 acceptors) arranged in a tetrahedral symmetry. Hydrogen (H) bond formation requires that 2 nearest neighbor molecules point respectively a donor and an acceptor towards each other. A number of nonbonding configurations is allowed, to account for H bond directionality. Bond weakening occurs (the bond energy is increased of some fraction) whenever a third molecule is placed near a formed bond. The latter feature basically mimics the fact that too closely packed water molecules disfavor H bonding. Let us notice that, while bonding properties are equivalent to those of the Bell model³⁴, the weakening criterion is different. The Roberts-Debenedetti model is quite appealing in that it has been shown to predict not only some of real water thermodynamic anomalies, such as the temperature of maximum density, but also a liquid-liquid phase separation in the supercooled region, and a second critical point. Nevertheless, the distinction between donors and acceptors is likely to be not so crucial to the physics of water. Therefore, in a previous paper⁴¹, we have investigated a simplified version of the model (without donor/acceptor distinction), showing that the same basic properties could be reproduced. Here we extend the simplified model to deal with aqueous solutions, working out solvation thermodynamics for an inert (apolar) solute. Our purpose is to verify whether the model is able to reproduce also the main features of hydrophobicity. This analysis might be interesting also in view of investigations on mixtures of water with more complex chemical species, such as polymers. We shall carry out the analysis by means of a generalized first-order approximation on a tetrahedral cluster, which has been verified to be quite accurate for the neat water model⁴¹.

II. THE MODEL

Let us introduce the model. Molecules are placed on the sites of a body-centered cubic lattice, whose structure is sketched in Fig. 1. A site may be empty or occupied by a water molecule (w) or by a solute molecule (s). An attractive potential energy $-\epsilon_{xy} < 0$ is assigned to any pair of nearest neighbor (NN) sites occupied by molecules of species x, y , where x and y can take the values w, s. This is the ordinary Van der Waals contribution. Water molecules possess four equivalent arms that can form H bonds, arranged in a tetrahedral symmetry, so that they can point towards 4 out of 8 NNs of a given site. There is no distinction between donors and acceptors, so that

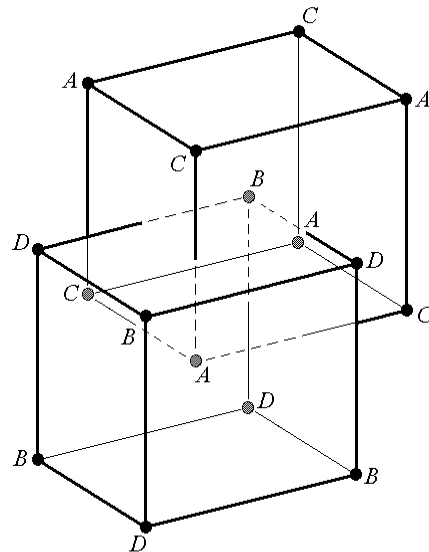


FIG. 1: Two conventional cells of the body-centered cubic lattice: A, B, C, D denote 4 interpenetrating face-centered cubic sublattices.

a H bond is formed whenever two NN molecules have a bonding arm pointing to each other, yielding an energy $-\eta < 0$. It is easily seen that water molecules have only 2 different configurations in which they can form H bonds (see Fig. 2). We assume that w more configurations are allowed, in which water molecules cannot form bonds (w is related to the bond-breaking entropy). Moreover, we assign an energy increase $\eta c_x/6$, with $c_x \in [0, 1]$, for each of the 6 sites closest to a formed bond (i.e., 3 out of 6 second neighbors of each bonded molecule), occupied by an x molecule. A bond surrounded by 6 molecules of species x contributes an energy $-\eta(1 - c_x)$. As far as water molecule are concerned, the weakening parameter mainly accounts for the fact that H bonds are most favorably formed when water molecules are located at a certain distance, larger than the optimal Van der Waals distance. Therefore, if too many molecules are present, the average distance among them is decreased, and hydrogen bonds are (on average) weakened. Moreover, the presence of an external molecule may perturb the electronic density, resulting in a lowered H bond strength as well. A weakening parameter for the solute (c_s) takes into account possible perturbation effects for a generic chemical species, even if in the following we shall mainly consider an ideally inert solute with $c_s = 0$.

The hamiltonian of the system can be written as a sum over irregular tetrahedra, whose vertices lie on 4 different face-centered cubic sublattices, shown in Fig. 1. One of such tetrahedra is shown in Fig. 3(a). We have

$$\mathcal{H} = \frac{1}{6} \sum_{\langle \alpha, \beta, \gamma, \delta \rangle} \mathcal{H}_{i_\alpha i_\beta i_\gamma i_\delta}, \quad (1)$$

where \mathcal{H}_{ijkl} is a contribution which will be referred to as tetrahedron hamiltonian, and the subscripts $i_\alpha, i_\beta, i_\gamma, i_\delta$

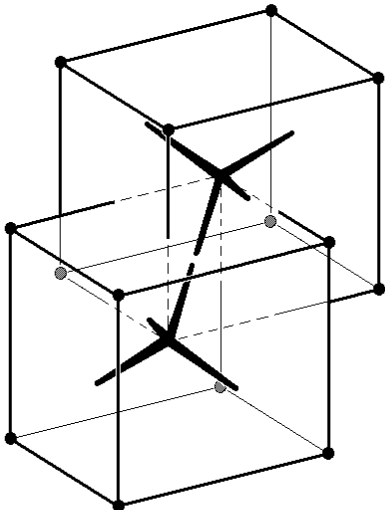


FIG. 2: Two model molecules forming a H bond. The lower molecule is in the $i = 1$ configuration, the upper one is in the $i = 2$ configuration.

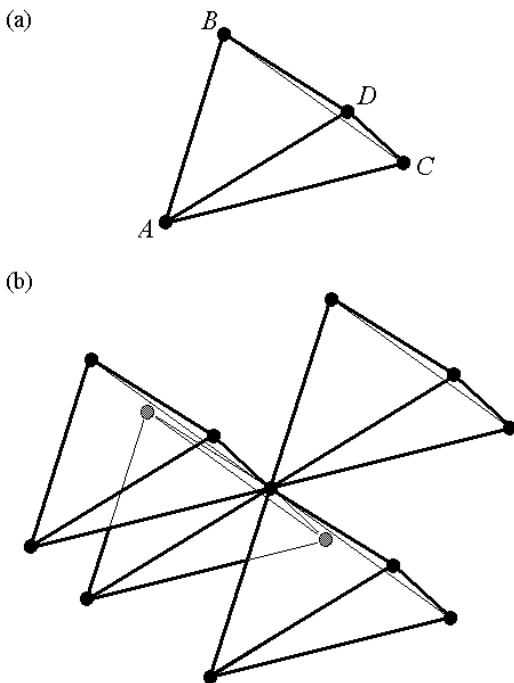


FIG. 3: (a) Basic cluster (irregular tetrahedron): A, B, C, D denote sites in the 4 corresponding sublattices. $AB, BC, CD,$ and DA are NN pairs; AC and BD are second neighbor pairs. (b) Husimi tree structure corresponding to the generalized first order approximation on the tetrahedron.

label site configurations for the 4 vertices $\alpha, \beta, \gamma, \delta,$ respectively. Possible site configurations are: “empty” ($i = 0$), “bonding water” (site occupied by a water molecule in one of the 2 orientations which can form

TABLE I: Site configuration labels (i), with corresponding multiplicities (w_i) and occupation numbers for water ($n_{w,i} = 1$) and solute ($n_{s,i} = 1$).

i	0	1	2	3	4
w_i	1	1	1	w	1
$n_{w,i}$	0	1	1	1	0
$n_{s,i}$	0	0	0	0	1

bonds: $i = 1, 2$; see Fig. 2), “nonbonding water” (site occupied by a water molecule in one of the w orientations which cannot form bonds: $i = 3$), “solute” (site occupied by a solute molecule: $i = 4$). Assuming that $(i, j), (j, k), (k, l),$ and (l, i) refer to NN pair configurations, the tetrahedron hamiltonian reads

$$\mathcal{H}_{ijkl} = H_{ijkl} + H_{jkli} + H_{klij} + H_{lijk}, \quad (2)$$

where

$$H_{ijkl} = -\epsilon_{xy} n_{x,i} n_{y,j} - \eta h_{ij} \left(1 - c_x \frac{n_{x,k} + n_{x,l}}{2} \right), \quad (3)$$

$n_{x,i}$ is an occupation variable for the x species, defined as in Tab. I, while h_{ij} are bond variables, defined as $h_{ij} = 1$ if the pair configuration (i, j) forms a H bond, and $h_{ij} = 0$ otherwise. Here and in the following, we understand that repeated x, y indices are to be summed over their possible values w, s . Let us also assume that i, j, k, l (in this order) denote configurations of sites placed on, say, A, B, C, D sublattices respectively. If A, B, C, D are defined as in Fig. 1, we can define $h_{ij} = 1$ if $i = 1$ and $j = 2$, and $h_{ij} = 0$ otherwise. With the above assumptions, the tetrahedron hamiltonian is independent of the orientation, that is of the arrangement of A, B, C, D on its vertices. Let us notice that both Van der Waals ($-\epsilon_{xy} n_{x,i} n_{y,j}$) and H bond energies ($-\eta h_{ij}$), which are 2-body terms, are split among 6 tetrahedra, whence the $1/6$ prefactor in Eq. (1). On the contrary, the 3-body weakening terms ($\eta c_x h_{ij} n_{x,k} / 6$) are split between 2 tetrahedra, thus the $1/6$ factor is absorbed in the prefactor, while a $1/2$ factor is left in the tetrahedron hamiltonian.

III. FIRST ORDER APPROXIMATION

We perform the investigation by means of a generalized first order approximation on a tetrahedral cluster. In the previous paper⁴¹, we have introduced the approximation in the variational approach⁴⁴, as a particular choice of the largest clusters left in the entropy expansion (basic clusters). Such a choice, sometimes denoted as cluster-site approximation⁴⁵ (the only clusters to be taken into account in the expansion are basic clusters and single sites), has not only the advantage of high simplicity, but also of relative accuracy, which has been recognized for different models^{31,45}. The basic clusters are a number of irregular tetrahedra, namely, 4 out of 24 tetrahedra sharing a

given site, as sketched in Fig. 3. This choice turns out to coincide with the (generalized) first order approximation (on a tetrahedron), also equivalent to the exact calculation on a Husimi lattice⁴⁶, whose (tetrahedral) building blocks are just arranged as in Fig. 3(b). In the present paper, we employ the latter approach, which, not having to treat cluster probability distributions explicitly, is numerically more convenient.

Husimi lattice thermodynamics can be studied exactly, in a numerical way, by solving a suitable recursion relation⁴⁶, since the system is locally treelike. First of all, we have to choose, as a Husimi lattice hamiltonian, the following expression

$$\mathcal{H}' = \sum_{\langle \alpha, \beta, \gamma, \delta \rangle} \mathcal{H}_{i_\alpha i_\beta i_\gamma i_\delta}, \quad (4)$$

obtained from Eq. (1) by understanding that the sum runs over tetrahedra in the treelike system only, and removing the $1/6$ prefactor. Let us notice that the latter change is required, in order to obtain equal internal energy densities (internal energies per site) for the Husimi lattice and the ordinary lattice system. If we denote the tetrahedron configuration probability by p_{ijkl} , and assume that it is equal on every tetrahedron, the internal energy density can be written as

$$u = \sum_{i=0}^4 w_i \sum_{j=0}^4 w_j \sum_{k=0}^4 w_k \sum_{l=0}^4 w_l p_{ijkl} \mathcal{H}_{ijkl}, \quad (5)$$

where w_i is the multiplicity of the i -th site configuration, equal to w for the nonbonding configuration of water ($i = 3$) and equal to 1 otherwise (see Tab. I). One then has to define partial partition functions (PPFs) in the following way. Let us consider a single branch of a Husimi tree, made up of tetrahedral blocks, and a corresponding partial hamiltonian, obtained by Eq. (4) with the sum restricted to tetrahedra in the branch. The PPF Q_i is defined as a sum of the Boltzmann weights of the partial hamiltonian over the configurations of the branch minus the base site (that is why the PPF depends on a site configuration variable i). Working in the grand-canonical ensemble, as we are interested in, we also have to take into account chemical potential contributions, which is done by replacing the tetrahedron hamiltonian \mathcal{H}_{ijkl} with

$$\tilde{\mathcal{H}}_{ijkl} = \mathcal{H}_{ijkl} - \mu_x \frac{n_{x,i} + n_{x,j} + n_{x,k} + n_{x,l}}{4}, \quad (6)$$

where the usual convention on repeated indices holds. Let us notice that of course the PPF tends to infinity in the thermodynamic limit, that is for an “infinite generation branch”, therefore it is convenient to define a normalized PPF $q_i \propto Q_i$, for instance in such a way that

$$\sum_{i=0}^4 w_i q_i = 1. \quad (7)$$

In this way, q_i represents the i -th configuration probability that the base site would have if it were not attached to any other branch.

Let us now consider again the single branch of our Husimi tree. In the infinite generation limit, and in the hypothesis of a homogeneous system, the subbranches attached to the first tetrahedral block should be equivalent to the main one, so that one can write the recursion relation

$$q_i = y^{-1} \sum_{j=0}^4 w_j \sum_{k=0}^4 w_k \sum_{l=0}^4 w_l e^{-\tilde{\mathcal{H}}_{ijkl}/T} (q_j q_k q_l)^3, \quad (8)$$

where the sums run over configuration variables in the tetrahedron except i , T is the temperature expressed in energy units (whence entropy will be expressed in natural units), and y is a normalization constant, imposed by Eq. (7). The recursion relation can be iterated numerically to determine a fixed point, representing the PPF of a branch whose base site lies in the bulk of the Husimi tree (generally denoted as Husimi lattice). Husimi lattice properties are equivalent to those obtained by the cluster-site approximation⁴⁶. We can compute the site probability distribution p_i , by considering the operation of attaching 4 equivalent branches to the given site. We obtain

$$p_i = z^{-1} q_i^4, \quad (9)$$

where

$$z = \sum_{i=0}^4 w_i q_i^4 \quad (10)$$

provides normalization. We can also compute the tetrahedron probability distribution, by considering the operation of attaching 3 equivalent branches to each site of a given tetrahedron, yielding

$$p_{ijkl} \propto e^{-\tilde{\mathcal{H}}_{ijkl}/T} (q_i q_j q_k q_l)^3, \quad (11)$$

where of course the proportionality constant is determined by normalization. From the knowledge of the tetrahedron probability distribution $\{p_{ijkl}\}$ one can compute the thermal average of every observable in the first order approximation, the internal energy density by Eq. (5), and the grand-canonical free energy by Eq. (10) in Ref. 41. According to Eq. (31) in Ref. 46, the latter can be also related to normalization constants as

$$\omega = -T (\ln y - 2 \ln z), \quad (12)$$

where y is the normalization constant of the recursion relation (8) and z is given by Eq. (10). Finally, the entropy density can be computed as

$$s = \frac{u - \mu_x \rho_x - \omega}{T}, \quad (13)$$

where $u - \mu_x \rho_x$ has formally the same expression as u in Eq. (5), with the tetrahedron hamiltonian \mathcal{H}_{ijkl} replaced by $\tilde{\mathcal{H}}_{ijkl}$.

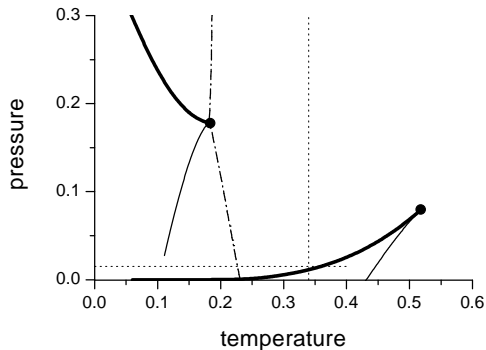


FIG. 4: Pressure (P/η) vs temperature (T/η) phase diagram for pure water with $\epsilon_{ww}/\eta = 0.3$, $c_w = 0.5$, and $w = 20$. Thick solid lines denote (first order) phase transitions; circles are critical points. Thin (solid and dash-dotted) lines denote the spinodals and the Kauzmann line, respectively. Dotted straight lines denote constant temperature ($T/\eta = 0.34$) and constant pressure ($P/\eta = 0.015$) “cuts”, corresponding to the solution phase diagrams, reported in Fig. 6.

IV. RESULTS

In order to investigate the model properties, we fix a set of parameters, as a result of several attempts. First of all, we take $\epsilon_{ww}/\eta = 0.3$. This value of water-water Van der Waals interaction is equal to the one employed for the very detailed analysis by Roberts et al.⁴³, though a bit larger than previously employed by us⁴¹. Anyway, this choice accounts for the greater binding energy of hydrogen bonds with respect to Van der Waals interactions. As far as the multiplicity of nonbonding water configurations is concerned, we set $w = 20$ (as in the previous work), which mimics the high directionality of hydrogen bonds. For neat water, it is necessary to set this parameter large enough to let anomalous properties appear, but further increase does not change qualitatively the phase diagram and the thermodynamic properties. As far as the weakening parameters are concerned, for water we choose $c_w = 0.5$, which, given the other parameter values, corresponds to a situation without a reentrant spinodal, in agreement with most recent molecular dynamics results³.

A. Pure water properties

Since the parameter choice is slightly different from the former work⁴¹, we first reconsider neat water properties, taking the limit $\mu_s \rightarrow -\infty$. This analysis is mainly meant to show that the model behavior still remains consistent with a “realistic” phase diagram, that is, with several experimental evidences as well as simulation predictions. In fact, we have observed that relatively small variations in parameter values may give rise to quite dramatic changes

in the phase behavior⁴¹, as observed also in other models of water⁴⁷. The temperature-pressure phase diagram is reported in Fig. 4. Imposing homogeneity, our analysis includes both thermodynamically stable and metastable (supercooled) phases, even if stability is not investigated. Let us notice that pressure can be determined as $P = -\omega$, where ω is the grand-canonical potential per site, introduced in the previous section. We have assumed the volume per site equal to unit, so that pressure is expressed in energy units. The appropriate order parameter is the density, i.e., the probability ρ_w that a site is occupied by a water molecule, which can be evaluated from the formula

$$\rho_x = \sum_{i=0}^4 w_i p_i n_{x,i}. \quad (14)$$

We find two different first order transition lines, terminating in two different critical points. The positively sloped line, at lower pressures, corresponds to the coexistence of a very low density phase and a high density phase, and represents the ordinary vapor-liquid transition. The other one, negatively sloped and placed at higher pressures, corresponds to coexistence between the high density liquid and a lower density one. The related critical point may reasonably represent the so-called second critical point, which has been conjectured and observed in simulations, and of which also some experimental evidences have been given. As one could expect, the low density liquid turns out to be more hydrogen bonded than the high density one. We find a density maximum as a function of temperature for liquid coexisting with vapor (and at constant pressure as well), and the temperature of maximum density slightly decreases upon increasing pressure, as observed in experiments.

We also report the liquid phase spinodals and the Kauzmann line. Details about the (semi-analytical) calculation of spinodals, which allows to determine density response functions as well, are given in the previous paper⁴¹. The limit of stability of the liquid phase (spinodal) is the locus at which the metastable liquid ceases to be a minimum of (a variational form of) the free energy, and becomes a saddle point. On the contrary, the Kauzmann line is the locus at which the liquid phase entropy vanishes, and corresponds to the ideal glass transition. It can be easily determined numerically. As previously mentioned, we do not observe a reentrance of the liquid-vapor spinodal in the positive pressure half-plane, which is actually a possibility of our model, for a different parameter choice, namely, for higher values of the weakening parameter. The reentrant spinodal scenario was one of the conjectures invoked to explain thermodynamic anomalies of liquid water, and in particular of the divergent-like behavior of response functions in the supercooled regime^{48,49}, even if at the moment the second critical point scenario is believed to be more realistic³.

For the present parameter choice, in our model the critical point lies just above the Kauzmann line, while

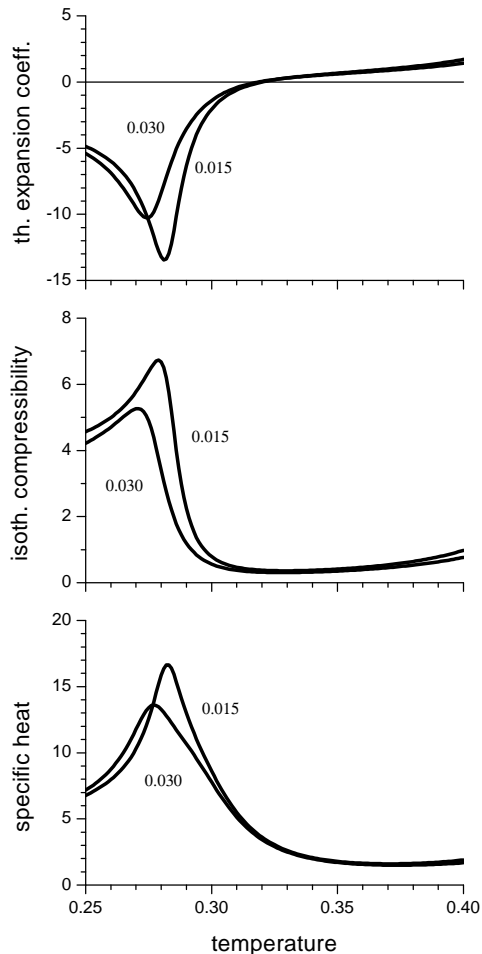


FIG. 5: Response functions at constant pressure ($P/\eta = 0.015, 0.030$) for pure liquid water as a function of temperature (T/η), for $\epsilon_{ww}/\eta = 0.3$, $w = 20$, and $c_w = 0.5$. From top to bottom, we show the isobaric thermal expansion coefficient ($\eta\alpha_P$), the isothermal compressibility ($\eta\kappa_T$), and the specific heat (c_P). Numerals beside each plot denote pressure values.

most of the high-low density liquid transition lies in the negative entropy region. This is consistent with the experimental observation of two different forms of amorphous ice in this region, while the “underlying” liquid phase is just an extrapolation of the equation of state for the liquid. The Kauzmann line displays a cusp (actually a slight discontinuity), while intersecting the high-low density liquid transition. It is noticeable that a similar feature has been predicted also by a recent analysis of the potential energy landscape of simulated water, performed by Sciortino and coworkers⁵⁰, on the basis of the inherent structure theory.

Let us also report the density response functions and the specific heat of the liquid at constant pressure $P/\eta = 0.015, 0.030$, roughly corresponding to $1/5, 2/5$ of the liquid-vapor critical pressure. Also for these calculations,

details are reported in Ref. 41. We find anomalous behavior, qualitatively similar to that of real liquid water. The first response function we consider is the thermal expansion coefficient $\alpha_P = (-\partial \ln \rho / \partial T)_P$, which, from statistical mechanics, is known to be proportional to the entropy-volume cross-correlation. For ordinary fluids, α_P is always positive, i.e., the local entropy and the local specific volume are positively correlated. On the contrary, for our model α_P (Fig. 5, top panel) is anomalous. As temperature is lowered, the expansion coefficient vanishes (at the temperature of maximum density), and then becomes negative. Of course, we do not observe a really divergent behavior of this coefficient, but a pronounced peak instead. Let us notice that, upon increasing pressure, the peak is observed to become broader, indicating that the liquid is becoming more normal, in agreement with experiments. The trend of the isothermal compressibility $\kappa_T = (\partial \ln \rho / \partial P)_T$ is also anomalous (Fig. 5, middle panel). For a typical liquid, κ_T decreases as one lowers temperature, because it is proportional to density fluctuations, whose magnitude decreases upon decreasing temperature. On the contrary, we observe that κ_T , once reached a minimum, begins to increase upon decreasing temperature. The constant pressure specific heat $c_P = (T\partial s / \partial T)_P$ (Fig. 5, bottom panel) displays a completely analogous behavior, with the minimum occurring at a higher temperature.

B. Solution properties

Let us now consider an ideal inert solute molecule, with no Van der Waals interaction with water ($\epsilon_{ws} = 0$), nor with other solute molecules ($\epsilon_{ss} = 0$), and no weakening effect on H bonds ($c_s = 0$). As a first analysis of the model mixture of water with this kind of (hydrophobic) solute, let us investigate phase diagrams at constant temperature and constant pressure, corresponding to the “cuts” reported in Fig. 4. We take into account, as a composition variable, the solute molar fraction, defined as

$$x_s = \frac{\rho_s}{\rho_w + \rho_s}, \quad (15)$$

where ρ_w and ρ_s are determined by Eq. (14). In Fig. 6 (top panel), we report a constant temperature phase diagram, computed at $T/\eta = 0.34$. We can observe a first order transition between a water-rich and a solute-rich phase, which arises continuously from the vapor-liquid transition of neat water, as solute concentration is increased. To determine this transition, we have fixed several different values of water chemical potential μ_w , then we have determined numerically the value of solute chemical potential μ_s , for which both phases had the same pressure $P = -\omega$. The phase-separated (coexistence) region occupies large part of the diagram, that is, the molar fraction of solute which can be dissolved into water, without giving rise to phase separation, is very small. The

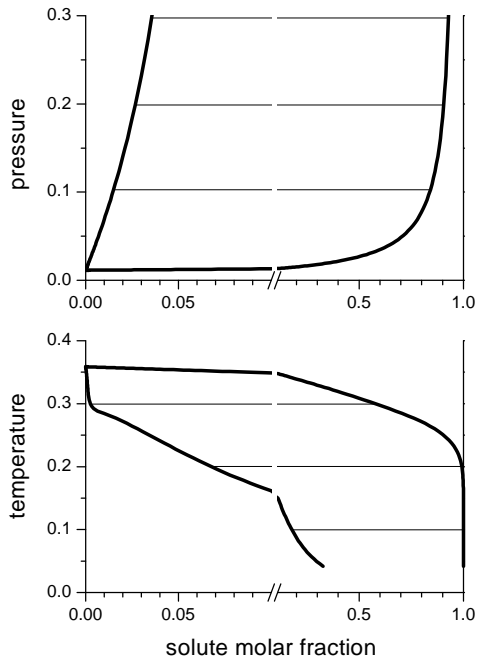


FIG. 6: Constant temperature ($T/\eta = 0.34$, top panel) and constant pressure ($P/\eta = 0.015$, bottom panel) phase diagrams for a mixture of water ($\epsilon_{ww}/\eta = 0.3$, $c_w = 0.5$, $w = 20$) with an ideal inert solute ($\epsilon_{ws} = \epsilon_{ss} = 0$, $c_s = 0$). Thick lines denote pure phase boundaries; thin lines connect coexisting phases and denote phase-separated regions.

behavior is very similar to that of an ordinary solution of two disaffine chemical species (at a temperature higher than the critical one for the solute), with no peculiar anomaly related to the hydrophobic effect. Notice that actually we cannot observe any phase transition for neat solute ($x_s = 1$), because we have described it as a perfect gas, with $\epsilon_{ss} = 0$. We have also computed a constant pressure phase diagram at $P/\eta = 0.015$, which we have reported in Fig. 6 (bottom panel). Here, to compute the transition, we have adjusted numerically both chemical potentials μ_w and μ_s to impose equality between pressures of both phases and the reference one. As expected, also in this case we observe no phase transition for pure solute, whereas a clearly anomalous behavior is observed for the water-rich phase boundary. Upon decreasing temperature, near $T/\eta \approx 0.31$, the slope of this curve begins to change rapidly. Such a behavior gives rise to an absorption coefficient x_s^w/x_s^s (the superscripts denoting the water-rich and the solute-rich phase, respectively) with a minimum around $T/\eta \approx 0.34$, well above the temperature of maximum density at that pressure (see Fig. 5). This is typical signature of hydrophobic effect¹⁸.

Let us now turn to the transfer properties of a single molecule in water, that is, to a dilute solution. Large amounts of experimental data are available for this case⁹. According to the Ben-Naim standard⁹, a transfer process

(for a chemical species x) can be characterized by means of the pseudo-chemical potential μ_x^* , related to the ordinary chemical potential μ_x by the formula

$$\mu_x = \mu_x^* + T \log \rho_x. \quad (16)$$

The use of pseudo-chemical potentials is meant to remove translational entropy contributions, which are not directly related to the solvation process. The solvation free energy per molecule Δg_x^* , that is, the free energy of transfer for a molecule x from the gas phase to the liquid phase, can then be defined as

$$\Delta g_x^* = \mu_x^{*l} - \mu_x^{*g}, \quad (17)$$

where μ_x^{*l} and μ_x^{*g} denote pseudo-chemical potentials in the liquid and gas phase, respectively. If the gas and liquid phases coexist in equilibrium, the ordinary chemical potentials for the given species must be equal, so that we obtain

$$\Delta g_x^* = -T \ln \frac{\rho_x^l}{\rho_x^g}, \quad (18)$$

where ρ_x^l and ρ_x^g denote densities for the x species in the two phases. Derived quantities, of interest in experiments, are the solvation entropy

$$\Delta s_x^* = - \left. \frac{\partial \Delta g_x^*}{\partial T} \right|_P, \quad (19)$$

the solvation enthalpy

$$\Delta h_x^* = \Delta g_x^* + T \Delta s_x^*, \quad (20)$$

and the solvation heat-capacity

$$\Delta c_{P_x}^* = \left. \frac{\partial \Delta h_x^*}{\partial T} \right|_P. \quad (21)$$

In principle, we should distinguish between derivatives taken at constant pressure (as stated by definition) or along the liquid-vapor equilibrium curve. In particular, we could not even use Eq. (18), because we would move out of the equilibrium curve. Nevertheless, we have verified that the difference between the two sets of results is negligible, in agreement with experimental observations⁹, and one can usually take the “equilibrium” derivative without further care.

Let us start studying solvation properties for the ideal inert solute, in the framework of our model. Water parameters are fixed as in the previous case. The temperature trends of the free energy, entropy, and enthalpy of transfer are given in Fig. 7a; the transfer heat capacity in Fig. 7c. In order to compare with experimental data^{8,9}, also reported in Fig. 7b and 7d, respectively, all quantities are evaluated at liquid-vapor coexistence, and for very low solute density with respect to water density (dilute solution limit). In practical calculations, we have adjusted numerically water and solute chemical potentials, in order to impose the equilibrium condition (equal

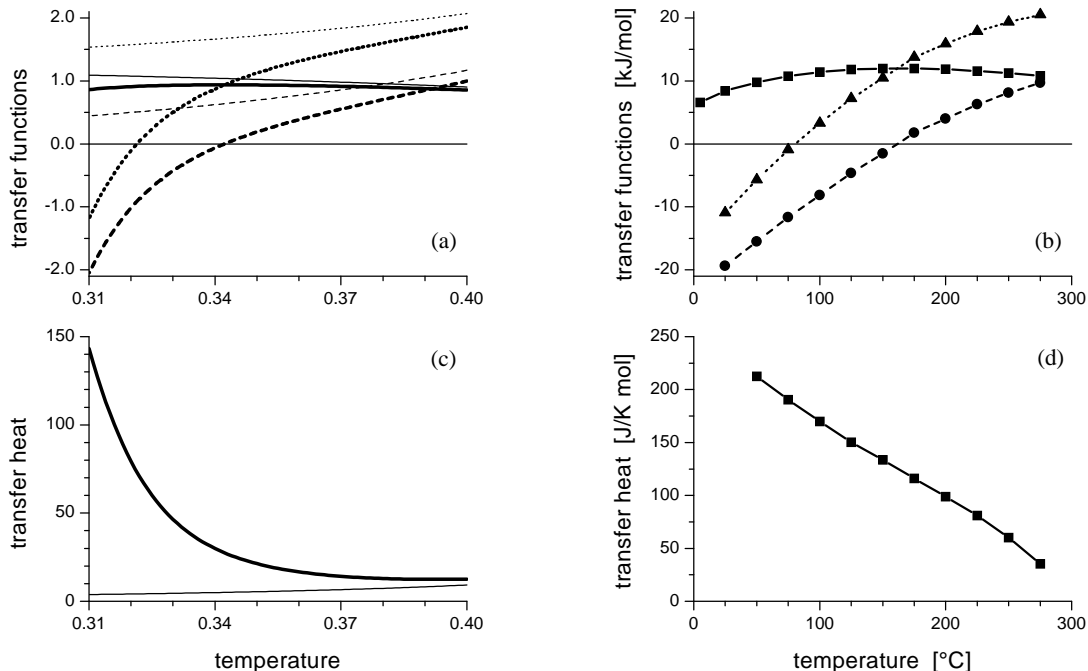


FIG. 7: (a) Transfer energy functions (E/η) vs temperature (T/η) for an ideal inert molecule in water at liquid-vapor coexistence: $E = \Delta g_s^*$ (solid line), $E = T\Delta s_s^*$ (dashed line), and $E = \Delta h_s^*$ (dotted line). (b) Corresponding experimental data for solvation of argon into water⁹. (c) Transfer heat capacity (Δc_P^*) vs temperature (T/η) for an ideal inert molecule. (d) Corresponding experimental data for argon⁹. Thin lines in (a) and (c) denote transfer quantities for nonbonding water.

pressure) between liquid and vapor, and to fix the solute molar fraction. Nevertheless, we have also verified that, only for the perfectly inert solute, concentration does not affect the results at all, so that we could also set an arbitrary value for the solute chemical potential. As shown in the previous section, our parameter set for pure water corresponds to a liquid-vapor critical temperature $T/\eta \approx 0.52$, and to a temperature of maximum density for the liquid phase around $T/\eta \approx 0.32$, at low pressure. Therefore, in order to represent roughly the experimental temperature range (between 0°C and 300°C) we report model results between $T/\eta = 0.31$ (just below the temperature of maximum density for pure liquid water) and $T/\eta = 0.40$ (about half way between the previous temperature and the critical temperature). Remarkably, it turns out that the model displays the defining features of hydrophobic solvation. The solvation free energy is positive and large, while the solvation entropy and enthalpy are negative at low temperatures and become positive upon increasing temperature. The solvation heat capacity is positive and large, and also the decreasing trend with temperature is basically reproduced. A slightly increasing trend at high temperature is related to the fact that we are approaching the liquid-vapor critical point. Negative solvation entropy at low (room) temperature is a clear indication that solute insertion into the mixture orders the system. The corresponding positive (unfavorable) contribution to free energy compensates a

negative (favorable) enthalpic contribution, giving rise to a positive solvation free energy. At higher temperature, enthalpic and entropic contributions change sign, but they still have the same compensating trend. The model also predicts two different temperatures at which the transfer enthalpy and entropy vanish (see Fig. 7a), as observed in experiments (Fig. 7b). The whole observed behavior is to be ascribed to the thermodynamics of H bonding and, in order to rationalize this fact in the model framework, we have also analysed transfer quantities, upon removing H bond interactions (see Fig. 7a,7c). As reasonable, the results are quite similar in the high temperature regime, where there is a high probability that H bonds are broken by thermal fluctuations, whereas they change more and more dramatically upon decreasing temperature, and, in particular, the regions of negative transfer entropy and enthalpy completely disappear. This facts confirm that H bonding is the key element for system ordering, upon insertion of an inert molecule. Accordingly, also the increasing trend of the heat capacity upon decreasing temperature is suppressed. The process is now dominated by enthalpy, with a large and positive transfer free energy (but without a maximum), and a positive transfer entropy. Transfer quantities now behave qualitatively as observed in solvation experiments of noble gas molecules in ordinary liquids^{9,51}, and are relatively independent of temperature. Actually, a water molecule for which H bond formation has been “turned

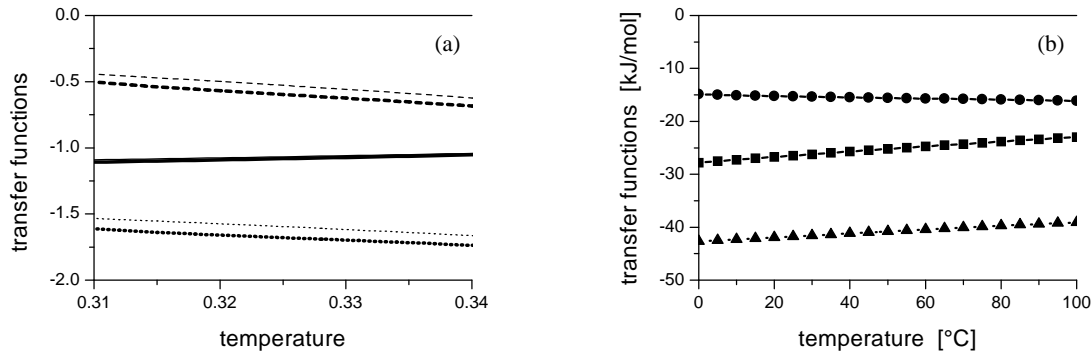


FIG. 8: (a) Transfer energy functions (E/η) vs temperature (T/η) for a water molecule into pure liquid water at liquid-vapor coexistence: $E = \Delta g_w^*$ (solid line), $E = T\Delta s_w^*$ (dashed line), and $E = \Delta h_w^*$ (dotted line). (b) Corresponding experimental data⁹. Thin lines in (a) denote transfer energies for nonbonding water.

off”, can be viewed as a nonpolar molecule with only Van der Waals interaction energy ϵ_{ww} .

Let us now consider also the solvation of water in its own pure liquid. Corresponding transfer quantities obtained by the model are displayed in Fig. 8a, where we have reduced the temperature interval, in order to compare with available experimental results⁹, reported in Fig. 8b. With respect to the inert molecule case, here absolute values of solvation free energy and entropy are considerably smaller. Enthalpy, rather than entropy, dominates the solvation process, while all quantities are relatively independent of temperature. These features characterize a regular transfer process, like the solvation of an ordinary fluid molecule from a gas phase into its pure liquid phase. In this case, upon removing H bond interactions (thin lines in Fig. 8a), very little changes are observed. Let us discuss two issues about these results. First, the fact that so little changes are caused by turning on or off H bonds can be rationalized on the basis of the microscopic model interactions. Insertion of a water molecule into pure liquid water should imply in principle the formation of new H bonds, but the model is such that insertion of a new water molecule also weakens other H bonds in its neighborhood, and the two effects nearly compensate each other. Second, let us notice that solvation enthalpy decreases upon increasing temperature, that is, the solvation heat capacity is negative, in contrast with experiments. We do not have an explanation for this fact, but we can observe that it is basically unchanged when H bonds are turned off, that is, when the model is reduced to describe a “regular” solvation process. This suggests that there is probably a limitation of the lattice description, that anyway has nothing to do with peculiarities of water. Indeed, the effect is quantitatively small, so that it is hidden by other large (enthalpic and entropic) effects, observed in the case of hydrophobic solvation.

C. “Nonideal” solute and entropy convergence

So far, we have always turned off all interactions involving solute molecules, except excluded volume. Here we report some results concerning the role of nonzero solute-water interaction parameters (ϵ_{ws} , c_s), still assuming that solute molecules have no relevant interaction with one another ($\epsilon_{ss} = 0$). In order to have a single parameter to be varied, we have performed our investigation for increasing values of the solute weakening parameter c_s , and defined solute-water interaction ϵ_{ws} according to the following proportionality condition

$$\epsilon_{ws}/\epsilon_{ww} = c_s/c_w. \quad (22)$$

At the beginning, we took this assumption as a simple trial, but the results we obtained were quite interesting, so that we have carried on with the analysis. As far as transfer free energies are concerned, we have observed a qualitatively unchanged behavior, with a broad maximum at some temperature, and free energy values getting smaller and smaller, upon increasing ϵ_{ws} and c_s . On the contrary, we have observed peculiar features concerning entropies, actually related to one another, which are displayed in Fig. 9a. Still upon increasing ϵ_{ws} and c_s , the temperature of zero entropy is progressively shifted towards higher values, while different entropy curves converge in a very narrow temperature range, relatively close to zero entropy temperatures. Moreover, entropy values at convergence are negative and relatively small. As one can observe in Fig. 9b, all of these features correspond remarkably well to phenomenology observed for the series of noble gases⁹, in particular the entropy convergence, which has attracted some interest, due to the fact that a similar effect has been observed for the entropies of protein unfolding⁵². Because of this unexpected result, we have tried and justified a posteriori the working hypothesis (22), and actually a naive explanation may be the following one. As a first approximation, different hydrophobic species, such as noble gases, may be viewed as hard

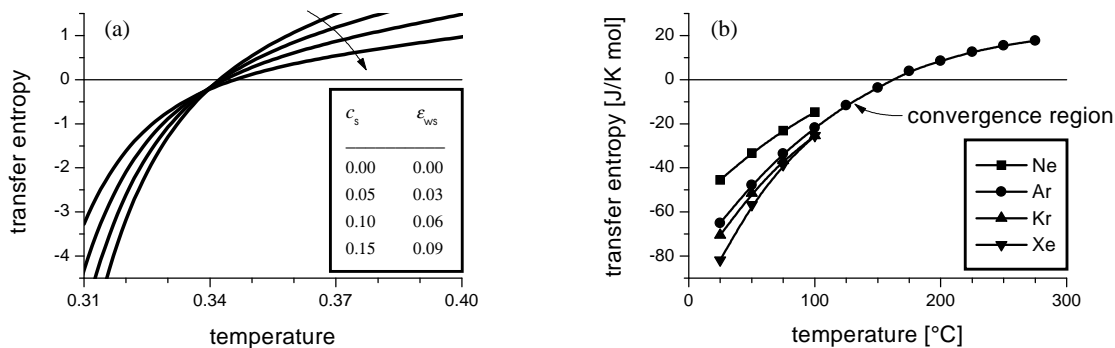


FIG. 9: (a) Transfer entropy (Δs_s^*) vs temperature (T/η) for a solute molecule into pure liquid water at liquid-vapor coexistence, for different solute parameter values, with $\epsilon_{ss} = 0$ and $\epsilon_{ws}/\epsilon_{ww} = c_s/c_w$. The arrow denotes increasing values of c_s and ϵ_{ws} . (b) Corresponding experimental data for noble gases⁹.

spheres distinguished by their diameter, that is their volume, only. In this way, the proportionality condition can be conceived as a trick that, in the framework of the lattice model, mimics the fact that “a fraction” c_s/c_w of the site occupied by the solute actually “behaves like water”. As a consequence, higher values of the ratio c_s/c_w should correspond to smaller solute molecules, which turns out to be consistent, comparing Figs. 9a and 9b. Let us notice also that, for parameter values as in Fig. 9a, the “fractions that behaves like solute” ($1 - c_s/c_w$) correlate well with the squares of the hard sphere diameters of the corresponding substances⁵³, which is consistent with the common assumption that hydrophobicity is proportional to exposed surface.

V. DISCUSSION AND CONCLUSIONS

In this paper we have considered a 3-dimensional lattice fluid model of water, which we had previously shown to exhibit realistic thermodynamic anomalies⁴¹, and extended the model to describe aqueous solutions. The motivation for this work resides mainly in the interest for the hydrophobic effect, whose relevance for biological processes such as protein folding, taking place in aqueous solutions, has been more and more recognized in the latest years. Moreover, a simplified but accurate modelling of water is an appealing issue, in view of investigations on such processes, because detailed water models may be extremely time consuming⁷.

As far as water is concerned, our model is a simplified version of a previous model proposed by Roberts and Debenedetti⁴⁰, without a distinction between hydrogen bond donors and acceptors. In the framework of this model, the microscopic description of water anomalies, is essentially based on the competition between an isotropic (Van der Waals like) interaction and an highly directional (H bonding) interaction, and on the difference between the respective optimal interaction distances. In the lat-

tice environment, the latter is taken into account by a trick, that is, the weakening effect of a water molecule near a formed bond. The same assumptions also accounts for possible perturbations of the electronic density, due to interaction with other water molecules. We have extended the weakening trick to take into account the presence of a different chemical species (solute), with no internal degrees of freedom (bonding arms). Calculations have been performed in a generalized first-order approximation on a tetrahedral cluster, which requires small computational effort, and had been shown to be quite accurate for the pure water model⁴¹.

Due to the fact that we have chosen slightly different interaction parameters for the present investigation, we have first analysed again pure water behavior. At constant pressure, the typical thermodynamic anomalies are reproduced, with a density maximum, and a minimum of isothermal compressibility and specific heat. In the ordinary temperature and pressure region, the temperature of maximum density decreases upon increasing pressure, as observed in experiments. Moreover, as far as the supercooled regime is concerned, there is still evidence of a second (metastable) critical point, which terminates a line of coexistence between two liquid phases at different densities. Let us recall that the pure water model could predict, for different values of the weakening parameter c_w , two different scenarios, that is, with or without a reentrant spinodal. The present parameter choice predicts a nonreentrant spinodal. The reentrant spinodal scenario was the first conjecture put forth to justify water anomalies, whereas the most recent and accurate molecular dynamics simulations of water suggest a scenario with a nonreentrant spinodal and a metastable liquid-liquid critical point³. As far as the critical point is concerned, in our calculation, it lies at some temperature just above the Kauzmann line, at which the configurational entropy vanishes, while the Kauzmann line displays a cusp upon crossing the metastable coexistence line. All of these features turn out to be in a remarkably

good agreement with the inherent state analysis of the potential energy landscape of simulated water, recently performed by Sciortino and coworkers⁵⁰.

As far as the solution model is concerned, we have mainly considered solutions of inert, that is, hydrophobic solutes. First of all, we have investigated phase diagrams for arbitrary solute concentration, pointing out a minimum of solubility as a function of temperature, as typical for hydrophobic solutions. We have investigated in more detail the dilute solution limit, at liquid-vapor equilibrium, for which many experimental data are available. Solvation quantities turn out to exhibit peculiar features that are believed to be the fingerprints of hydrophobicity. The solvation free energy is positive (unfavorable solvation), while entropy and enthalpy are negative at low temperatures and positive at high temperatures. The solvation heat capacity is large and decreases upon increasing temperature. These results compare qualitatively well with solvation experiments for noble gases in water. Let us notice that a previous lattice model by Besseling and Lyklema²⁴, based on a different description of water interactions, was also able to account for the qualitative behavior of free energy, enthalpy, and entropy of transfer. Nevertheless, it failed in reproducing the correct temperature trend of the transfer heat capacity, which, according to some authors⁷ is a key feature, revealing the cooperative nature of the hydrophobic effect. Let us recall, by the way, that the same difficulty about heat capacity is encountered by the information theory approach⁵⁴.

We have investigated explicitly on the effect of H bonding, in the framework of our model, performing calculations also when this interaction is completely turned off. In this case, we have obtained transfer quantities that approach the ones computed *with* H bonds at high temperatures, but that largely deviates from them upon decreasing temperature, that is, in the region where H bonding begins to dominate. In particular, we have observed that, while disaffinity between solute and solvent is left (the solvation free energy is still positive), this is mainly of enthalpic nature. Both the enthalpy and entropy of solvation remain positive at all temperatures, so that also the typical strong temperature dependence of hydrophobic solvation, disappears.

We have also taken into account the solvation process of water into its own pure liquid, for which experimental data are available. We have found qualitative agreement, as far as the values of transfer free energy, entropy and enthalpy are concerned, but we have observed some discrepancy in the temperature dependence of enthalpy, indicating a negative solvation heat capacity, in disagreement with experiments. We have verified that the same kind of discrepancy can be observed if H bonding is turned off, that is, for an ordinary lattice gas. Therefore, we suggest that the discrepancy is to be related to an intrinsic limitation of the lattice environment, that has nothing to do with peculiarities of the water model. The effect is

relatively small, so that it is completely invisible, when the dominant effect of H bonds is introduced.

Let us notice that the results concerning transfer quantities are qualitatively similar to those observed for a 2-dimensional lattice model recently investigated by us⁵⁵, which in turn is a simplified “lattice version” of the Mercedes Benz model investigated by Dill and coworkers. In spite of similarities in the experimental temperature range, there is one major difference between the two models. The 2-dimensional model is not able to account for the metastable critical point of water, probably due to impossibility of reproducing a high density ordered packing of water molecules. As a consequence, thermodynamic anomalies are entirely due to the presence of a reentrant spinodal, which is no longer believed to be a realistic scenario for real water³. In this sense, the present 3-dimensional model seems to provide a more coherent view of water thermodynamics, relating each other neat water anomalies and hydrophobic effect.

Moreover, we have shown that, with quite a reasonable assumption for the solute interaction parameters ϵ_{ws}, c_s (attempting to describe solutes of different volume in the lattice framework), the model is able to reproduce also the entropy convergence phenomenon, in a qualitatively correct way. Such a phenomenon has been theoretically described, for instance, by the simplified molecular theory of Debenedetti and coworkers¹⁷. Moreover, an almost quantitative explanation has been proposed by Pratt and coworkers⁵³, on the basis of the information theory approach, which we mentioned in the Introduction. In the cited work, the authors argue that entropy convergence, and in particular the negative entropy at convergence, are related to the weak temperature dependence of free volume fluctuations in liquid water, that is, isothermal compressibility. Although we cannot provide a clear explanation of why our lattice model, with the proportionality assumption (22), exhibits qualitatively correct behavior, let us notice that such result is somehow consistent with the previous explanation. In fact, entropy convergence occurs very close to the minimum of isothermal compressibility, as one can argue from Fig. 5, that is, in a region where compressibility is nearly constant, as a function of temperature. Nonetheless, the proportionality assumption (22) still remains not well justified.

Let us finally recall that our model, at least in the present treatment, is not able to provide microscopic structural details as simulations do, but its most appealing feature is simplicity. In the present paper we have shown that, in spite of this, the model yields a qualitatively coherent description of peculiar thermodynamics of water, not only as a pure substance but also as a solvent, and is consistent with predictions based on much more sophisticated models and simulations. Moreover, thanks to the 3-dimensional embedding, it may be suitable for quite a realistic analysis of more complex, for instance polymeric, solutes. We are going to report about such investigations in a forthcoming article.

-
- ¹ D. Eisenberg and W. Kauzmann, *The Structure and Properties of Water* (Oxford University Press, Oxford, 1969).
- ² F. Franks, ed., *Water: a Comprehensive Treatise* (Plenum Press, New York, 1982).
- ³ H. E. Stanley, S. V. Buldyrev, N. Giovambattista, et al., *J. Stat. Phys.* **110**, 1039 (2003).
- ⁴ H. S. Frank and M. W. Evans, *J. Chem. Phys.* **13**, 507 (1945).
- ⁵ A. Ben-Naim, *Hydrophobic interactions* (Plenum Press, New York, 1980).
- ⁶ K. A. Dill, *Science* **250**, 297 (1990).
- ⁷ N. T. Southall, K. A. Dill, and A. D. J. Haymet, *J. Phys. Chem. B* **106**, 521 (2002).
- ⁸ R. Crovetto, R. Fernández-Prini, and M. L. Japas, *J. Chem. Phys.* **76**, 1077 (1982).
- ⁹ A. Ben-Naim, *Solvation Thermodynamics* (Plenum Press, New York, 1987).
- ¹⁰ K. A. Dill, *Biochemistry* **29**, 7133 (1990).
- ¹¹ H. E. Stanley, S. V. Buldyrev, M. Canpolat, et al., *Physica A* **257**, 213 (1998).
- ¹² P. H. Poole, F. Sciortino, T. Grande, H. E. Stanley, and C. A. Angell, *Phys. Rev. Lett.* **73**, 1632 (1994).
- ¹³ F. H. Stillinger, *Science* **209**, 451 (1980).
- ¹⁴ M. W. Mahoney and W. L. Jorgensen, *J. Chem. Phys.* **112**, 8910 (2000).
- ¹⁵ H. E. Stanley, M. O. Barbosa, S. Mossa, et al., *Physica A* **315**, 281 (2002).
- ¹⁶ D. Paschek, *J. Chem. Phys.* **120**, 6674 (2004).
- ¹⁷ H. S. Ashbaugh, T. M. Truskett, and P. G. Debenedetti, *J. Chem. Phys.* **116**, 2907 (2002).
- ¹⁸ B. Widom, P. Bhimalapuram, and K. Koga, *Phys. Chem. Chem. Phys.* **5**, 3085 (2003).
- ¹⁹ P. Bruscolini and L. Casetti, *Phys. Rev. E* **64**, 051805 (2001).
- ²⁰ H. Reiss, H. L. Frisch, and J. L. Lebowitz, *J. Chem. Phys.* **31**, 369 (1959).
- ²¹ B. Lee, *Biopolymers* **31**, 993 (1991).
- ²² G. Hummer, S. Garde, A. E. García, A. Pohorille, and L. R. Pratt, *Proc. Natl. Acad. Sci.* **93**, 8951 (1996).
- ²³ A. Ben-Naim, *J. Chem. Phys.* **54**, 3682 (1971).
- ²⁴ N. A. M. Besseling and J. Lyklema, *J. Phys. Chem. B* **101**, 7604 (1997).
- ²⁵ R. Sharma and D. Kumar, *Phys. Rev. E* **58**, 3405 (1998).
- ²⁶ G. M. Bell and D. A. Lavis, *J. Phys. A* **3**, 427 (1970).
- ²⁷ G. M. Bell and D. A. Lavis, *J. Phys. A* **3**, 568 (1970).
- ²⁸ D. A. Lavis, *J. Phys. C* **6**, 1530 (1973).
- ²⁹ D. A. Lavis and N. I. Christou, *J. Phys. A* **12**, 1869 (1979).
- ³⁰ D. A. Huckaby and R. S. Hanna, *J. Phys. A* **20**, 5311 (1987).
- ³¹ C. Buzano, E. De Stefanis, A. Pelizzola, and M. Pretti, *Phys. Rev. E* **69**, 061502 (2004).
- ³² A. L. Balladares and M. C. Barbosa, *J. Phys. Cond. Matt.* **16**, 8811 (2004).
- ³³ A. B. de Oliveira and M. C. Barbosa, *J. Phys. Cond. Matt.* **17**, 399 (2005).
- ³⁴ G. M. Bell, *J. Phys. C* **5**, 889 (1972).
- ³⁵ G. M. Bell and D. W. Salt, *J. Chem. Soc., Faraday Trans. II* **72**, 76 (1976).
- ³⁶ D. A. Lavis and N. I. Christou, *J. Phys. A* **10**, 2153 (1977).
- ³⁷ P. H. E. Meijer, R. Kikuchi, and E. V. Royen, *Physica A* **115**, 124 (1982).
- ³⁸ S. Sastry, F. Sciortino, and H. E. Stanley, *J. Chem. Phys.* **98**, 9863 (1993).
- ³⁹ N. A. M. Besseling and J. Lyklema, *J. Phys. Chem.* **98**, 11610 (1994).
- ⁴⁰ C. J. Roberts and P. G. Debenedetti, *J. Chem. Phys.* **105**, 658 (1996).
- ⁴¹ M. Pretti and C. Buzano, *J. Chem. Phys.* **121**, 11856 (2004).
- ⁴² C. J. Roberts, A. Z. Panagiotopoulos, and P. G. Debenedetti, *Phys. Rev. Lett.* **77**, 4386 (1996).
- ⁴³ C. J. Roberts, G. A. Karayiannakis, and P. G. Debenedetti, *Ind. Eng. Chem. Res.* **37**, 3012 (1998).
- ⁴⁴ G. An, *J. Stat. Phys.* **52**, 727 (1988).
- ⁴⁵ W. A. Oates, F. Zhang, S. L. Chen, and Y. A. Chang, *Phys. Rev. B* **59**, 11221 (1999).
- ⁴⁶ M. Pretti, *J. Stat. Phys.* **111**, 993 (2003).
- ⁴⁷ T. M. Truskett, P. G. Debenedetti, S. Sastry, and S. Torquato, *J. Chem. Phys.* **111**, 2647 (1999).
- ⁴⁸ R. J. Speedy, *J. Phys. Chem.* **86**, 982 (1982).
- ⁴⁹ Q. Zheng, D. J. Durben, G. H. Wolf, and C. A. Angell, *Science* **254**, 829 (1991).
- ⁵⁰ P. T. F. Sciortino, E. La Nave, *Phys. Rev. Lett.* **91**, 155701 (2003).
- ⁵¹ R. H. Davies, A. G. Duncan, G. Saville, and L. A. K. Staveley, *Trans. Faraday Soc.* **63**, 855 (1967).
- ⁵² B. Lee, *Proc. Natl. Acad. Sci.* **88**, 5154 (1991).
- ⁵³ S. Garde, G. Hummer, A. E. García, M. E. Paulaitis, and L. R. Pratt, *Phys. Rev. Lett.* **77**, 4966 (1996).
- ⁵⁴ J. W. Arthur and A. D. J. Haymet, *J. Chem. Phys.* **110**, 5873 (1999).
- ⁵⁵ C. Buzano, E. De Stefanis, and M. Pretti, to be published in *Phys. Rev. E* (2005).